



Tidal driven nutrient exchange between mangroves and estuary reveals a dynamic source-sink pattern

Fenfang Wang ^a, Peng Cheng ^b, Nengwang Chen ^{a, b, *}, Yi-Ming Kuo ^c

^a Key Laboratory of the Coastal and Wetland Ecosystems, College of the Environment and Ecology, Xiamen University, Xiamen, 361102, China

^b State Key Laboratory of Marine Environment Science, Xiamen University, Xiamen, 361102, China

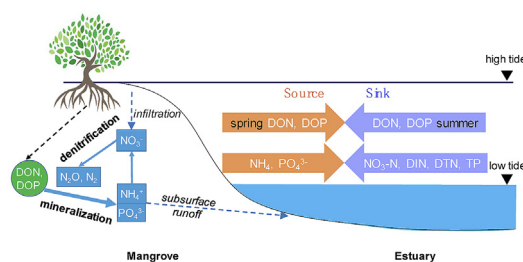
^c School of Environmental Studies, China University of Geosciences, Wuhan, 430074, China



HIGHLIGHTS

- Lateral nutrient flux across the mangrove-estuary interface were quantified.
- Hydrobiogeochemical processes determine the dynamic source-sink pattern over season.
- Mangroves decrease overall nutrient load and reduce estuary eutrophication.
- Upstream effluent discharge during ebb tide substantially increased nutrient export.

GRAPHICAL ABSTRACT



ARTICLE INFO

Article history:

Received 21 July 2020

Received in revised form

24 September 2020

Accepted 15 October 2020

Available online 21 October 2020

Handling Editor: Junfeng Niu

Keywords:

Wetlands

Nutrient fluxes

Zhangjiang estuary

Eutrophication

ABSTRACT

Nitrogen (N) and phosphorus (P) are vital nutrients regulating mangrove productivity and coastal ecosystems. Understanding of the nutrient cycling and interaction between mangroves and estuary is limited. Here we show tidal-driven nutrient exchange and a dynamic source-sink pattern across the mangrove-estuary interface. Lateral nutrient fluxes were quantified based on hourly concentrations observed at a tidal creek outlet during 2016–2018 and water mass estimated by a hydrodynamic model (FVCOM). The results of nutrient fluxes suggested that mangroves always serve as a source of ammonium ($\text{NH}_4\text{-N}$) and dissolved reactive P (DRP) to estuary, but as a strong nitrate sink ($\text{NO}_3\text{-N}$). Dissolved organic components (DON and DOP) shifted from net efflux (source) in spring to net influx (sink) in summer, likely due to the changing balance of P input and biological and physicochemical processes. Mangroves decreased the overall loading of dissolved inorganic N (DIN), dissolved total N (DTN) and total P (TP) to the estuary. Nevertheless, the effluents (aquaculture wastewater and domestic sewage) discharged from the upstream area during ebb tide increased the export of nutrients, especially $\text{NH}_4\text{-N}$ and DRP, offsetting the role of mangrove on mitigating coastal eutrophication.

© 2020 Elsevier Ltd. All rights reserved.

* Corresponding author. Key Laboratory of the Coastal and Wetland Ecosystems, College of the Environment and Ecology, Xiamen University, Xiamen, 361102, China.

E-mail address: nwchen@xmu.edu.cn (N. Chen).

1. Introduction

Mangrove forests, as one of the most economically valuable and biologically diverse ecosystems in coastal areas, provide a variety of ecological functions for society, including fisheries production, coastal protection and nutrient processing (Barbier et al., 2011; Camacho-Valdez et al., 2013; Atwood et al., 2017). Mangrove forests

can capture and store large amounts of carbon through the absorption of vegetation and the accumulation of sediments, contributing to the accumulation of “blue carbon” (Perera and Amarasinghe, 2019). Nutrients (especially nitrogen and phosphorus) in the mangrove system are important regulators of carbon cycling and mangrove productivity (Servais et al., 2019; Wang et al., 2019b). The cycling and export of nutrient across wetlands to estuary (and even ocean) contributes to the healthy or unhealthy (nutrient pollution, eutrophication, and harmful algal blooms) development of estuarine ecosystems (Whitehead and Crossman, 2012; Paerl et al., 2016). Understanding of the nutrient cycling and interaction between mangroves and estuary is essential to develop sound management strategies on coastal wetlands.

Studies on nutrient fluxes in mangrove systems have largely focused on the vertical dimension, including the interfaces of sediment-water, sediment-atmosphere and vegetation-atmosphere (Dittmar et al., 2006; Gleeson et al., 2013; Maher et al., 2013; Xiao et al., 2018; Santos et al., 2019). Given the rich organic matter and low conversion rate in mangrove forests, a large amount of dissolved material can be exported to adjacent estuarine systems (Taillardat et al., 2018). In contrast, only a few studies have so far focused on lateral carbon exchange between mangrove forest and coastal water, finding that many physicochemical processes can control carbon export, including porewater exchange, groundwater discharge, tidal pumping and potential biogeochemical reactions (Bergamaschi et al., 2012; Xiao et al., 2018; Call et al., 2019; Sadat-Noori and Glamore, 2019). However, the lateral fluxes of nutrients along the mangrove-estuary interface are understudied.

Mangroves are under great pressure due to human activities (e.g., agriculture, aquaculture, and urbanization) (Estoque et al., 2018; Munksgaard et al., 2019). Molnar et al. (2013) suggested that mineralization can be reduced and inorganic nitrogen cycling can be stimulated in mangrove systems affected by effluents compared to those without effluents input. Effluents were found to enhance both nitrification and denitrification leading to more release of greenhouse gases (N_2O , CO_2 and CH_4) (Chen et al., 2011; Zheng et al., 2018; Queiroz et al., 2019). However, there are few studies addressing the effects of effluents on the lateral nutrient export from mangrove to adjacent water.

This research investigated nutrient fluxes across a mangrove tidal creek (Yunxiao National Mangrove Nature Reserve) to adjacent estuary (Zhangjiang Estuary, Fujian province, southeast China). We conducted three time-series observations of nutrient concentrations and flow at the mouth of the creek during 2016–2018, and developed a nutrient flux model. The specific objectives of this study were to: (1) quantify nutrient (nitrogen and phosphorus species) fluxes across the mangrove-estuary interface; (2) reveal hydro-biogeochemical controls on the seasonal pattern of nutrient lateral exchange between mangrove and estuary; and (3) examine the impacts of upstream effluents (aquaculture wastewater and domestic sewage) on nutrient fluxes.

2. Materials and methods

2.1. Description of study site

The study was carried out in the National Mangrove Reserve and Zhangjiang Estuary ($117^{\circ}24' - 117^{\circ}30'E$, $23^{\circ}53' - 23^{\circ}56'N$) in Southeast China (Fig. 1). The dominant species in the mangrove forest are *Kandelia candel*, *Avicennia marina* and *Aegiceras corniculatum* (Zhou et al., 2010), with an increasing distribution of herbaceous *Spartina alterniflora* in the intertidal zone (Liu et al., 2017). The study area is subject to a subtropical monsoon climate, with an annual mean air

temperature of $22.8^{\circ}C$, and seasonal means of $21.4^{\circ}C$, $28.8^{\circ}C$, $25.5^{\circ}C$ and $15.9^{\circ}C$ in spring, summer, fall and winter respectively. The mean annual precipitation is about 1680 mm. The estuary experiences a semidiurnal tide with a large tidal range of 0.43–4.67 m (average 2.32 m) (Zhang et al., 2006). Upstream effluents, including aquaculture wastewater and domestic sewage, flow through dikes with a few sluices into mangrove creeks during low tide (Wang et al., 2010).

2.2. Tidal scale observation

The study targeted the interface of mangrove and estuary (Fig. 1). We carried out continuous hourly observations at a fixed station T (mouth of tidal creek) in July 2016 (warm season), April 2017 (cold season) and June 2018 (warm season) over a tidal cycle of 48 h, 25 h, and 25 h respectively. April represents the critical season for mangroves to start growing (Songsom et al., 2019), and also experiences increasing temperatures and nutrient supply from the river catchment as rainfall increases. In summer, high temperatures usually stimulate plant growth and microbial activities. This study focuses on these two important seasons to investigate the nutrient lateral exchange between mangrove and estuary and associated hydro-biogeochemical controls. We conducted one more summer observation in June 2018 to verify the patterns of nutrient fluxes across different years. Both July 2016 and June 2018 represent a summer climate but with somewhat different hydrodynamics.

Surface (0.5 m) water samples were collected and filtered in the field by a GF/F membrane ($0.7\ \mu m$), and then stored at $4^{\circ}C$ until analysis for nutrient concentrations within two days. Dissolved oxygen (DO), temperature ($^{\circ}C$), pH and salinity were measured *in-situ* using a WTW multi-parameter portable meter (Multi 3430, Germany). A Sea-Sun Tech CTD 48 M probe was installed in a fixed tube to measure water depth. Flow rate was measured by an *in-situ* acoustic Doppler current profiler (ADCP) (RDI WH 1200 kHz). Light Detection and Ranging was used to determine the elevation data in April 2017, which were used to determine the watershed boundary (Fig. S2).

2.3. Laboratory analysis

Filtrate was used to measure dissolved nutrient forms. NO_3-N , NO_2-N , NH_4-N and DRP were analyzed by segmented flow automated colorimetry (San++ analyzer, Germany) with the methods of cadmium reduction-naphthalene ethylenediamine spectrophotometry, naphthalene ethylenediamine spectrophotometry, indophenol blue spectrophotometry and molybdenum blue spectrophotometry respectively. Dissolved total nitrogen (DTN) and phosphorus (DTP) were determined as NO_3-N and DRP following oxidization with 4% alkaline potassium persulfate. Dissolved inorganic nitrogen (DIN) was summed from NO_3-N , NO_2-N and NH_4-N . Dissolved organic nitrogen (DON) was the difference between DTN and DIN and dissolved organic phosphorus (DOP) was the difference between DTP and DRP. The filtered membranes were used to measure total suspended materials (TSM) and total particulate phosphorus (TPP). More information about nutrient measurements are shown in Supporting Information Text S1.

2.4. Water flux estimation

The hourly water flux across the watershed boundary was calculated by the primitive equations, unstructured-grid, Finite-Volume Community Ocean Model (FVCOM) (Chen et al., 2006). The modeled tidal elevation was validated using observation data at a tidal gauge (station DS) at the mouth of Dongshan Bay (Fig. S3) and

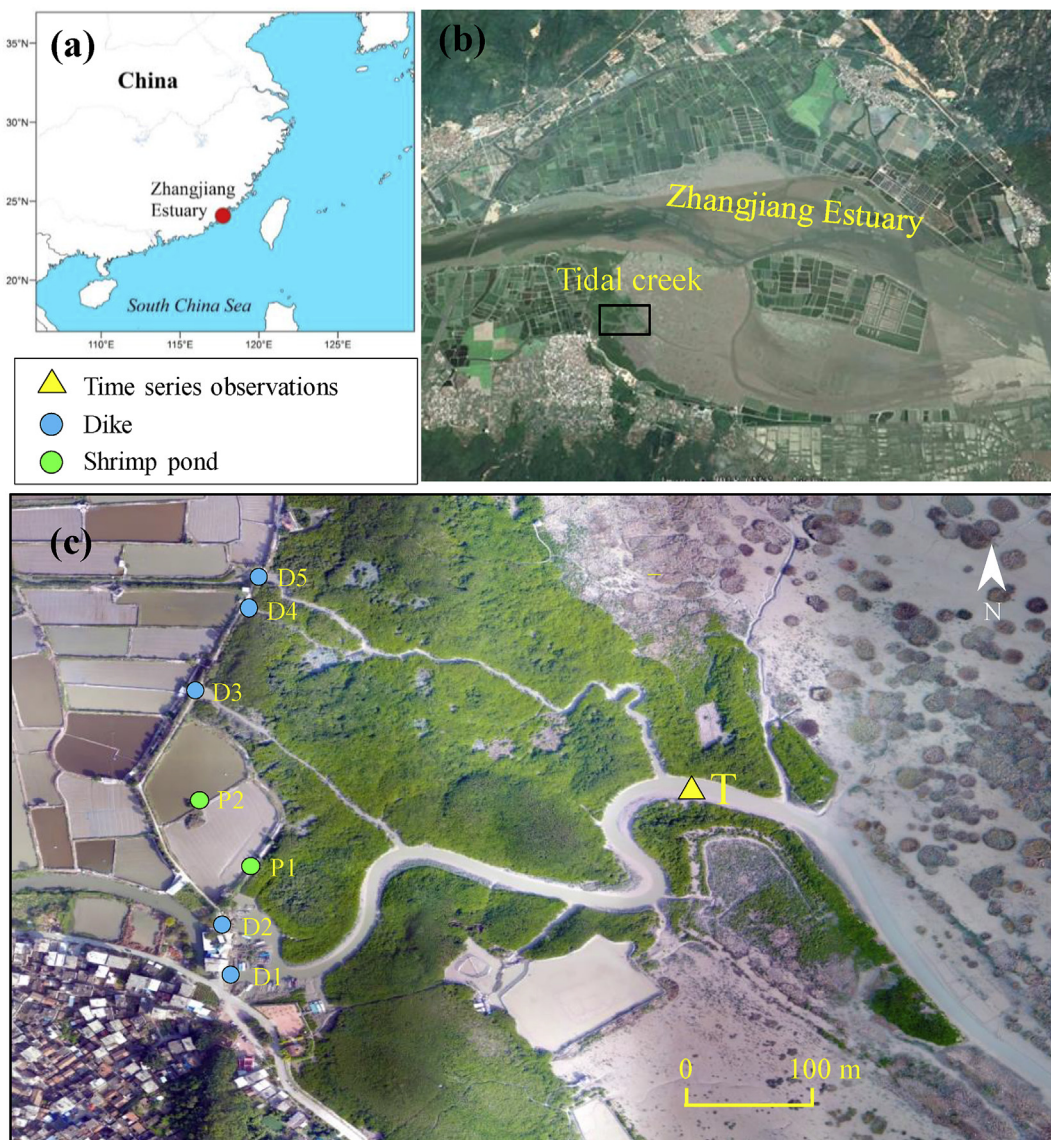


Fig. 1. Map of study area showing sampling sites (adapted from Wang et al., 2019a). D1-D5 are dikes discharging effluents to tidal creek. P1 and P2 are shrimp ponds. Time series observations were performed at fixed station T (mouth of tidal creek).

the fixed station T at the mouth of tidal creek (Fig. 1). More information about FVCOM model and the model validation are shown in Supporting Information (Fig. S3-S5, Text S2).

2.5. Data analysis and statistics

Water flux calculated by the FVCOM model and time-series concentrations of nutrients at the mouth of the tidal creek (station T) were used to estimate nutrient fluxes across the mangrove-estuary interface by equation (1).

$$F = \left(\sum_{i=0}^n C_i \times Q_i \right) / A / 1000 \quad (1)$$

where F is net fluxes ($\text{mg N m}^{-2} \text{h}^{-1}$) over a tidal cycle. Positive values are efflux from mangroves, and negative values are influx to mangroves. C_i is the hourly concentration of nutrient (mg L^{-1}) at site T in Fig. 1 (c). Nutrient concentrations showed good conservative mixing behaviors with salinity, indicating that C_i can

represent the average concentration across the mangrove-estuary boundary. Q_i ($\text{m}^3 \text{s}^{-1}$) is the average hourly water discharge across the boundary. A (m^2) means the catchment area of mangrove forest.

Uncertainty analysis of nutrient fluxes was carried out by setting water flux simulated errors by the FVCOM model as $\pm 10\%$, $\pm 20\%$ and $\pm 30\%$ in both high and low tides. More information about the analysis are shown in Text S3.

The partition coefficient of P (K_d) represents the partitioning of P between the dissolved (DTP) and particulate phase (TPP) and its particle reactivity. K_d was calculated by equation (2).

$$K_d = C_p / (C_d \times \text{SPM}) \quad (2)$$

In order to assess the influence of upstream effluents on nutrient fluxes during ebb tide, the observed concentrations were corrected to values without effluents for comparison. The method of correction is detailed in Supporting Information (Text S4 and Fig. S1).

3. Results

3.1. Hydrodynamic characteristics

Water level changed with tidal cycles (Fig. 2), ranging from -1.44 to 1.34 m, -1.44 to 1.83 m and -1.34 to 1.43 m in July 2016, April 2017 and June 2018, respectively. Flow rate exhibited high variability between the three observations ($P < 0.05$). The average flow rates during flood and ebb tides were largest in June 2018 (0.198 and 0.225 m s^{-1}), followed by April 2017 (0.164 and 0.126 m s^{-1}) and July 2016 (0.100 and 0.086 m s^{-1}). Averaged water temperature was 30.7 °C, 23.4 °C, and 29.3 °C in June 2018, April 2017 and July 2016.

Water fluxes during flood tide were larger than ebb tide ($P < 0.05$) (Fig. 2a–c). The peak water flux in July 2016 was 40.63 $\text{m}^3 \text{s}^{-1}$ with an average of 16.90 $\text{m}^3 \text{s}^{-1}$ during flood tide and 30.02 $\text{m}^3 \text{s}^{-1}$ with an average of 10.16 $\text{m}^3 \text{s}^{-1}$ during ebb tide. The average fluxes in June 2018 (18.03 and 12.98 $\text{m}^3 \text{s}^{-1}$ during flood and ebb tide) were close to July 2016, but the water fluxes in April 2017 were largest, peaking at 65.39 $\text{m}^3 \text{s}^{-1}$ (average 30.75 $\text{m}^3 \text{s}^{-1}$) during flood tide and 38.08 $\text{m}^3 \text{s}^{-1}$ (average 17.11 $\text{m}^3 \text{s}^{-1}$) during ebb tide.

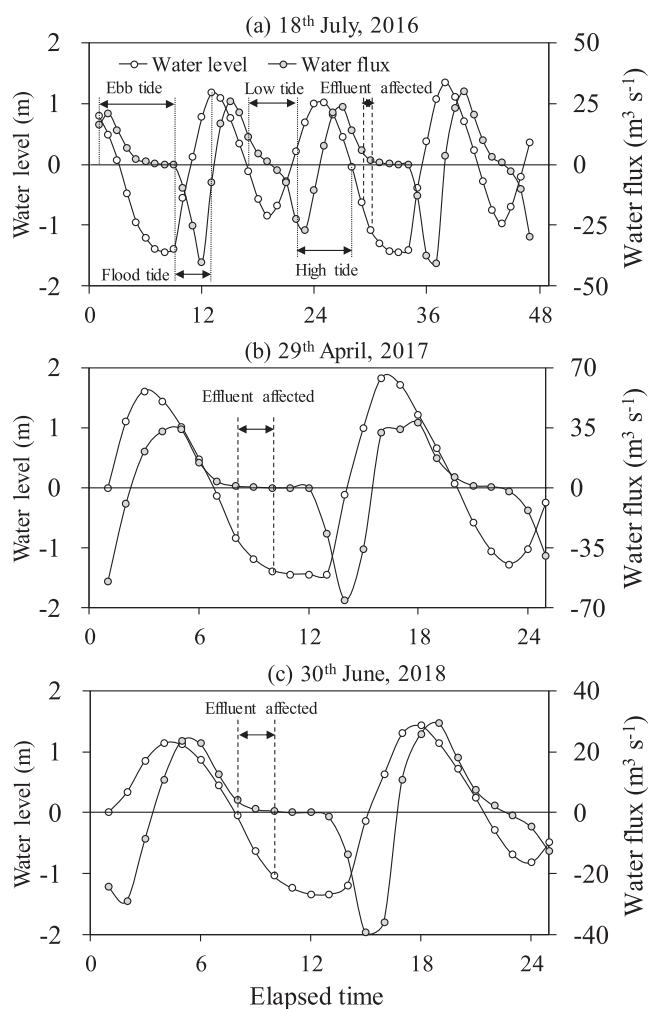


Fig. 2. Tidal variation of water level and water flux (a–c) starting on July 18th, 2016, April 29th, 2017 and June 30th, 2018. The periods of flood tide, ebb tide, high tide, low tide and effluent affected periods are marked in (a), (b) and (c). Water level shown as the deviation (anomaly) of the observed water depth from the average value.

3.2. Nutrient dynamics in mangrove tidal creek

The concentration and composition of nutrients varied regularly with the tidal cycles (Fig. 3). Average $\text{NH}_4\text{-N}$ in April 2017 were higher than those in July 2016 and June 2018, and the concentrations in low tide ($40.3\text{--}113.8$ $\mu\text{mol L}^{-1}$) were much higher than those in high tide ($21.3\text{--}51.3$ $\mu\text{mol L}^{-1}$). $\text{NO}_3\text{-N}$ in April 2017 were higher than those in July 2016, and the concentrations in low tide (75.0 and 136.1 $\mu\text{mol L}^{-1}$) were much lower than in high tide (113.2 and 147.5 $\mu\text{mol L}^{-1}$). However, there was an exception in June 2018, when $\text{NO}_3\text{-N}$ in low tide (130.4 $\mu\text{mol L}^{-1}$) were slightly higher than those in high tide (125.3 $\mu\text{mol L}^{-1}$). Average DRP in April 2017 was higher than in July 2016 but lower than in June 2018, while TPP had the maximum concentration in July 2016 and the minimum concentration in April 2017. Both DRP and TPP had higher concentrations in low tide ($4.1\text{--}9.8$ and $6.1\text{--}8.9$ $\mu\text{mol L}^{-1}$) compared to high tide ($3.6\text{--}5.4$ and $2.3\text{--}3.7$ $\mu\text{mol L}^{-1}$).

$\text{NO}_3\text{-N}$ was the dominant species (37%–57%) of DTN, followed by DON (26%–31%) and $\text{NH}_4\text{-N}$ (11%–31%), while $\text{NO}_2\text{-N}$ had the smallest shares. The dominant species of P were DRP (36.9%–65.5%) and TPP (26.7%–57.2%), while the DOP fraction was minor (3.5%–10.5%). During ebb tide, the fractions of $\text{NH}_4\text{-N}$ and TPP increased gradually while $\text{NO}_3\text{-N}$ and DRP decreased, but there was a contrary tendency during flood tide (Fig. 4). Accordingly, the average fractions of $\text{NH}_4\text{-N}$ and TPP were higher during low tide than high tide ($P < 0.05$), while $\text{NO}_3\text{-N}$ was higher in high tide period ($P < 0.05$).

Effluents discharged from upstream areas had a great influence on nutrient concentrations. In effluents-affected periods (low tide), the average concentrations of $\text{NH}_4\text{-N}$, DON, DRP and DOP were 60%, 49%, 122% and 96% higher respectively than those of the unaffected periods. In contrast, $\text{NO}_3\text{-N}$ was 28% lower than the unaffected samples, with the exception of June 2018 when it was 60% higher.

3.3. Nutrient fluxes across the creek-estuary interface

The magnitude and direction of nutrient fluxes (without effluent) across the tidal creek-estuary interface varied among nutrient species and between seasons (Fig. 5). $\text{NH}_4\text{-N}$ was exported from mangrove tidal creek to estuary (efflux), and the net flux in April 2017 (2.18 $\text{mg m}^{-2} \text{h}^{-1}$) was larger than in June 2018 (1.37 $\text{mg m}^{-2} \text{h}^{-1}$) and July 2016 (0.44 $\text{mg m}^{-2} \text{h}^{-1}$). In contrast, $\text{NO}_3\text{-N}$ was imported from estuary to mangrove (influx), and the net flux in April 2017 (-3.84 $\text{mg m}^{-2} \text{h}^{-1}$) was much smaller than in July 2016 and 2018 (-11.94 and -13.23 $\text{mg m}^{-2} \text{h}^{-1}$). DON fluxes shifted from efflux in April 2017 (0.59 $\text{mg m}^{-2} \text{h}^{-1}$) to influx in July 2016 (-0.14 $\text{mg m}^{-2} \text{h}^{-1}$) and June 2018 (-6.21 $\text{mg m}^{-2} \text{h}^{-1}$). DIN had influx in all three observations, and the fluxes in July 2016 and 2018 (-12.15 and -20.43 $\text{mg m}^{-2} \text{h}^{-1}$) were larger than in April 2017 (-1.95 $\text{mg m}^{-2} \text{h}^{-1}$). DTN always showed a net input to mangrove with the maximum and minimum flux in June 2018 and April 2017 (-20.43 and -1.37 $\text{mg m}^{-2} \text{h}^{-1}$).

DRP was net exported from mangrove to estuary, and the flux in April 2017 (0.33 $\text{mg m}^{-2} \text{h}^{-1}$) was slightly smaller than in June 2018 (0.45 $\text{mg m}^{-2} \text{h}^{-1}$) and July 2016 (0.42 $\text{mg m}^{-2} \text{h}^{-1}$). DOP was net imported to mangrove in July 2016 and 2018 (-0.68 and -0.98 $\text{mg m}^{-2} \text{h}^{-1}$) but became a net export to estuary in April 2017 (0.11 $\text{mg m}^{-2} \text{h}^{-1}$). TPP had influx in June 2018 and April 2017 (-0.08 and -1.95 $\text{mg m}^{-2} \text{h}^{-1}$) while small efflux or influx in July 2016 considering the uncertainty of water fluxes estimation. The overall TP had influx, and the flux in April 2017 (-1.51 $\text{mg m}^{-2} \text{h}^{-1}$) was larger than July 2016 and June 2018 (-0.12 and -0.61 $\text{mg m}^{-2} \text{h}^{-1}$).

The effluent discharged from upstream areas affected nutrient

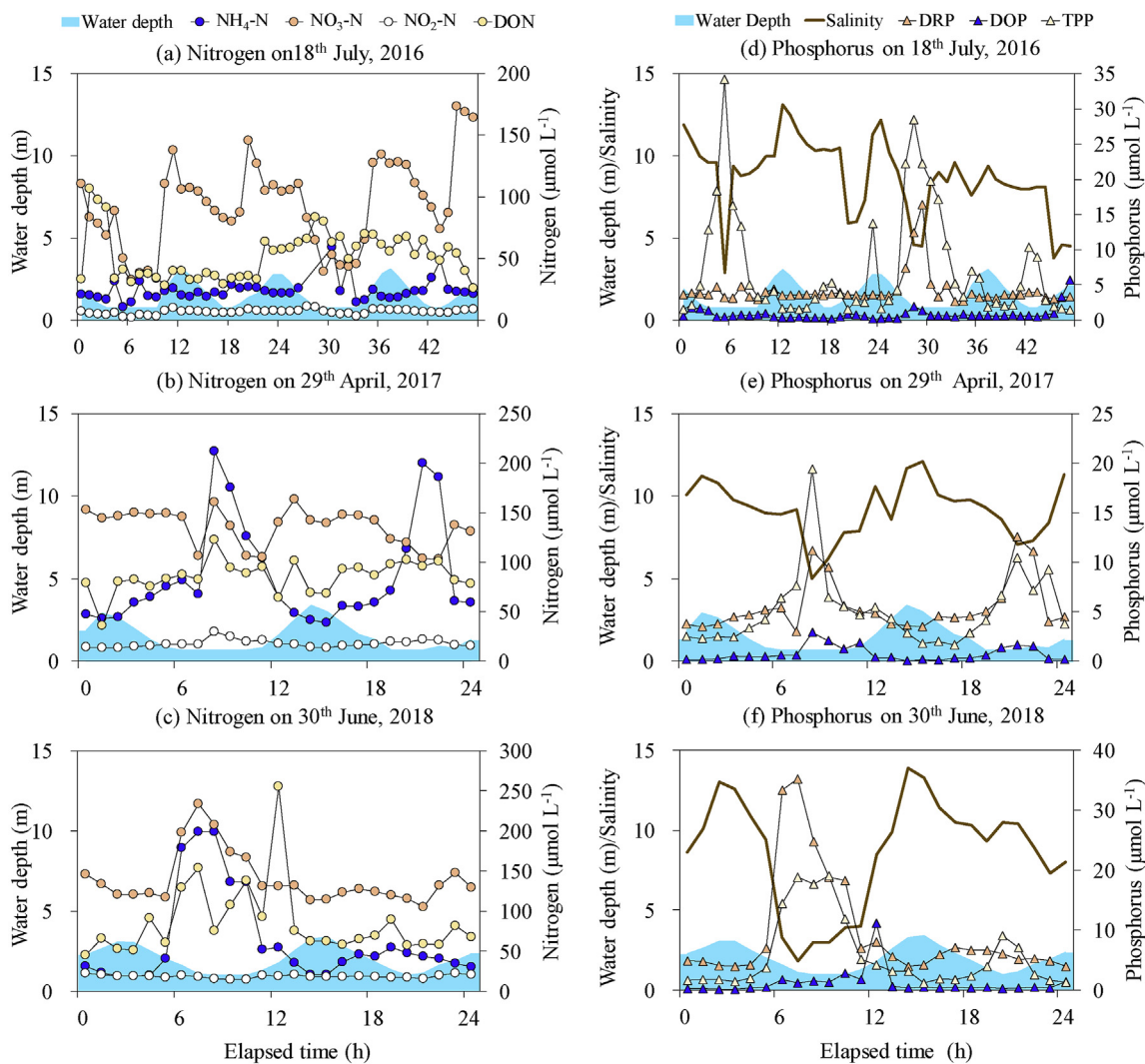


Fig. 3. Tidal variations of water depth, salinity and concentrations of nitrogen (a–c) and phosphorus (d–f) starting on July 18th, 2016, April 29th, 2017 and June 30th, 2018

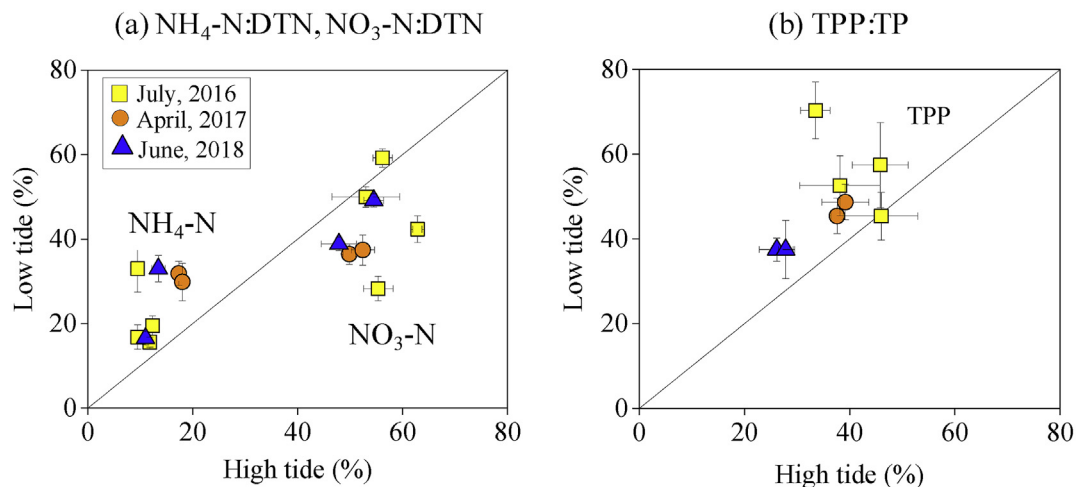


Fig. 4. Average fractions of $\text{NH}_4\text{-N}$ and $\text{NO}_3\text{-N}$ of DTN (a), and TPP of TP (b) during low tide against high tide periods. Error bar indicates one standard deviation.

fluxes during ebb tide, particularly in July 2016 and June 2018 (Fig. 6). In the two summer cases, the DTN fluxes with effluent from mangrove creek to estuary were 3% and 29% higher than the

corrected fluxes excluding effluent influence. The contribution of effluents on the increase of $\text{NH}_4\text{-N}$ fluxes was most significant among N species with increases of 28% and 68% (July and June

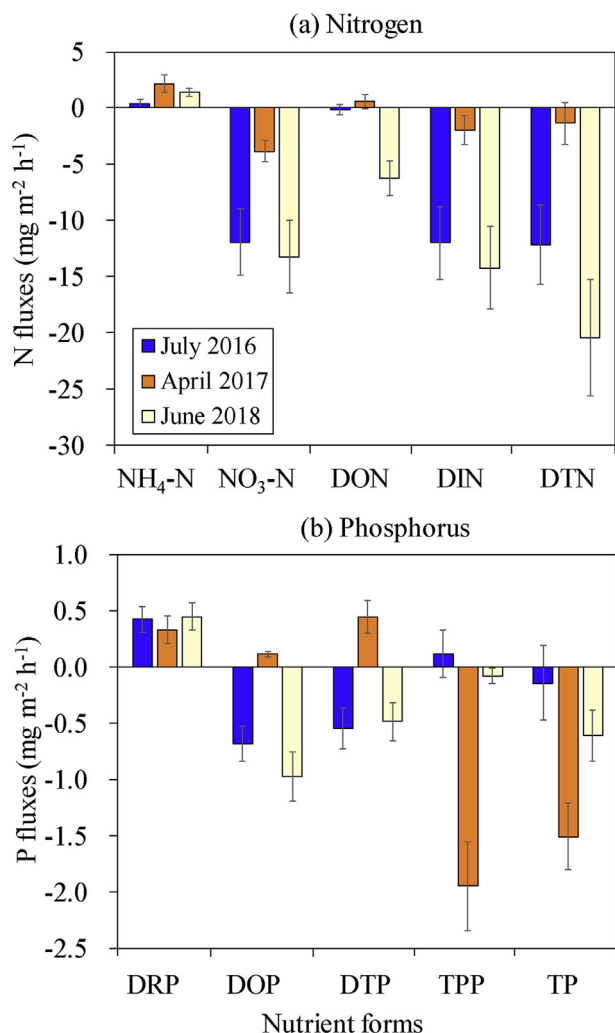


Fig. 5. Net nutrient fluxes (without effluent) in July 2016, April 2017 and June 2018. Positive values indicate nutrient efflux from mangrove, and negative values indicate nutrient influx to mangrove. Error bar is one standard deviation of estimated fluxes considering water flux simulated errors scenarios ($\pm 10\%$, $\pm 20\%$ and $\pm 30\%$) by FVCOM (see Text S3).

respectively), followed by DON with increases of 3% and 39%, while DTP fluxes increased by 1.28 and 9.58 $\text{mg m}^{-2} \text{h}^{-1}$ (17% and 78% higher respectively). DRP fluxes were 16% and 85% higher, accounting for the greatest increase in P fluxes. In spring case of April 2017, the fluxes of both N and P during the effluent affected period (ebb tide) changed little (Fig. 6).

4. Discussion

4.1. Tidal driven nutrient exchange and major biogeochemical processes shaping the source-sink pattern

Tides are the main hydrologic mechanism driving the lateral exchange of nutrients between mangroves and estuarine water. Nutrient fluxes were positively correlated with water fluxes across the mangrove-estuary interface ($p < 0.05$) during flood tide except for DOP and TPP (Table S1 and Fig. S6), suggesting nutrient export was mainly driven by tidal exchange.

The biogeochemical processes of nutrients occurring within the mangrove system also influence whether nutrients are supplied to the estuary or retained. Our previous study concluded that there was strong mineralization in the mangrove sediments at the creek

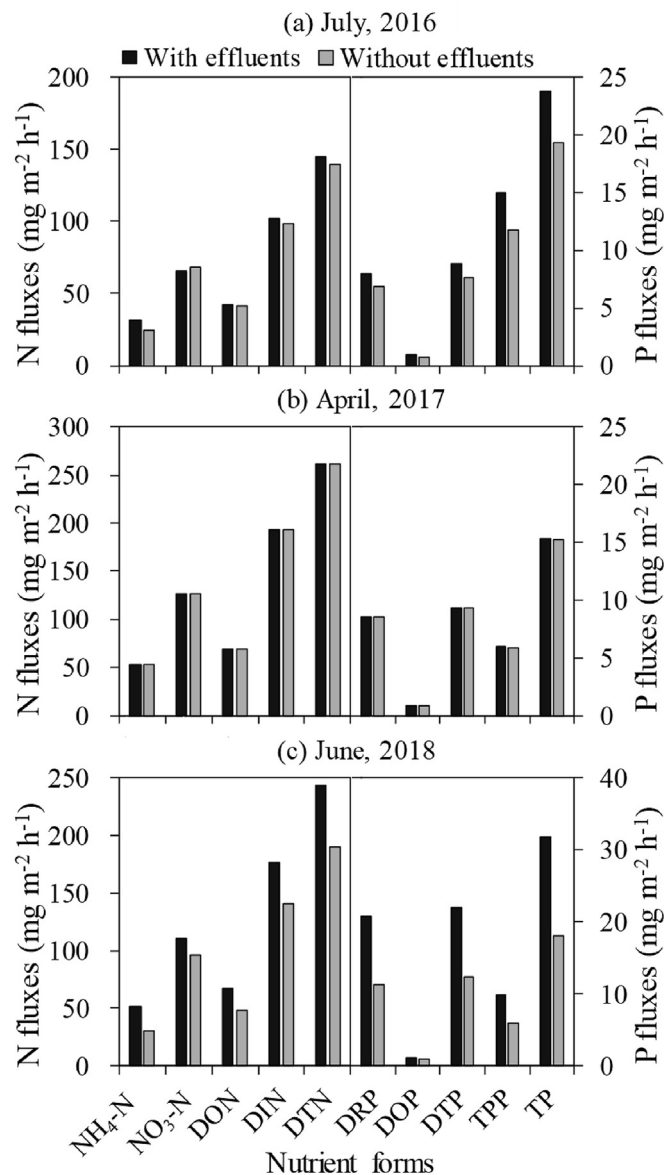


Fig. 6. Comparison on nutrients export during ebb tide with and without effluent discharge in July 2016, April 2017 and June 2018.

slope, which resulted in high concentration of inorganic matter ($\text{NH}_4\text{-N}$, DIC, etc.) in sediment pore water (Wang et al., 2019a). In this study, the average concentration and fraction of $\text{NH}_4\text{-N}$ and DRP increased during ebb tides compared with flood tides (Figs. 3 and 4), and they had net effluxes in most tidal cycles (Table S1). These results confirm that mangrove sediment pore water is a source of $\text{NH}_4\text{-N}$ and DRP (products of organic matter mineralization) as these products can be discharged to the tidal creek during ebb tide by increased hydraulic forcing. Particles could affect $\text{NH}_4\text{-N}$ concentrations in water by adsorption and desorption. $\text{NH}_4\text{-N}$ can be released from particles in high-salinity water (Hopkinson et al., 1999; Weston et al., 2010). The salinity observed in our study ranged from 2 to 13 and TSM was low ($136 \pm 106 \text{ mg L}^{-1}$) in high tide period (high salinity). There was no obvious relationship between TSM and $\text{NH}_4\text{-N}$ (Fig. S7d-f). We therefore speculate that the effect of particles on $\text{NH}_4\text{-N}$ concentrations is relatively unimportant.

The ammonium released from the mangrove sediments

(porewater) can be partly oxidized to nitrite and nitrate and returned to the mangrove forest during flood tide with subsequent removal by denitrification. $\text{NO}_3\text{-N}$ penetrates into anaerobic sediments during high tide periods can be reduced by denitrification. As a result, the average concentration and fraction of $\text{NO}_3\text{-N}$ in the creek water decreased during ebb tides (Fig. 4). The discharge of sediment porewater with low $\text{NO}_3\text{-N}$ was also found to cause a dilution in the tidal creek during ebb tide (Wang et al., 2019a). The influx suggested that mangroves served as a $\text{NO}_3\text{-N}$ sink relative to the estuary. DIN had an influx from estuary to mangrove, largely due to large $\text{NO}_3\text{-N}$ removal and less ammonium addition in sediments. Although mangroves will always be a sink for bioavailable N on annual time scales, they can behave differently in different seasons (see discussion below).

The process of absorption and desorption during tidal cycling increased the complexity of TPP flux. Flooding water can increase re-suspension of sediments and particulate matter. The large K_d in July 2016 (Table S3) represents a stronger possibility of desorption of P, and the higher concentrations of TSM and TPP in ebb tide compared with flood tide supports the efflux from mangrove to estuary. K_d was smaller in June 2018 than April 2017 (Table S3), indicating that more phosphate was likely attached to the suspended sediments (Fig. S7c). In addition, the net water fluxes in April 2017 were much greater than in June 2018, explaining much more influx of TPP from estuary to mangrove.

Estuarine TPP can be trapped by mangrove roots and deposited during the high tide period when the flow rate decreases. All the values of K_d in flood tides were greater than in ebb tides (Table S3), indicating that estuarine TPP can be partially desorbed when it enters the mangrove due to decreasing pH and salinity. This desorption of TPP would subsequently export backwards as DRP during ebb tide. The concentration of organic nutrient (DON and DOP) is associated with the degradation of leaves, the absorption of plants, precipitation, atmospheric deposition and marine inputs (Maie et al., 2008; Kaiser et al., 2013; Valiela et al., 2018; Zhang et al., 2019). The results of this study show a balance between influx and efflux of DON in July 2016 and April 2017 but a significant sink in June 2018 (Fig. 5). A possible explanation for the 2018 observation is that the water fluxes and the concentrations of DON during high tide were larger than in low tide. DOP had a similar pattern with DON. The decomposition of organic matter and the utilization of nutrients by vegetation varied among seasons (see more discussion in 4.3).

Mangroves fringed along the estuary bank have an open boundary and the tidal water cannot totally go back by flowing into the tidal creek (Table S1). The imbalance of water fluxes (flood > ebb) might lead to underestimation of the fluxes of $\text{NH}_4\text{-N}$, DRP and other source species from mangrove to estuary during ebb tide, while the influx of $\text{NO}_3\text{-N}$ and other sink species from estuary to mangrove during flood ebb might be overestimated. Nevertheless, the concentrations in low tide versus high tide (Table S2) suggested that the concentrations of $\text{NH}_4\text{-N}$ and other source species were higher while $\text{NO}_3\text{-N}$ and other sink species were lower in the mangrove tidal creek than in the estuary. This source-sink pattern was always true even if water mass is imbalanced (i.e. larger flux in flood tide than ebb tide). The FVCOM model may under-estimates or over-estimates the water depth across tidal cycles (Fig. S5). Uncertainty analysis of nutrient fluxes further confirmed the source-sink pattern assuming a deviation of estimated water fluxes in a range of 10%–30% (Fig. 5 and Text S3).

4.2. Seasonality of nutrient fluxes showing a dynamic source-sink pattern

The lateral fluxes of nutrients exchanged across mangrove and

adjacent estuary were largely controlled by the nutrient balance between supply and the demand of mangrove plants and microorganisms in the mangrove sediments. The net import of $\text{NO}_3\text{-N}$ to mangrove was higher in summer (June, July) than in spring (April), but net export of $\text{NH}_4\text{-N}$ to estuary was larger in spring than summer (Fig. 5). Mangroves forests are highly efficient users of DIN forms from tidal waters, related to rapid plant uptake and an efficient conservation of DIN in sediment by microbial activity (Reis et al., 2017). Our previous study suggested that there was evident nitrification in mangrove surface sediments and strong denitrification in deep sediments (Wang et al., 2019a). High temperature usually stimulates $\text{NO}_3\text{-N}$ removal by microbial denitrification (Lee et al., 2011; Duan et al., 2019). As a result, the outwelling of $\text{NO}_3\text{-N}$ from mangrove sediments was small in summer, leading to relatively high $\text{NO}_3\text{-N}$ import. A few studies have shown that nutrient uptake and productivity likely increase with temperature in mangrove forests (Field, 1995; Chen et al., 2009). $\text{NH}_4\text{-N}$ was the most common DIN in mangrove sediments (Alongi et al., 1992), explaining the small outwelling of $\text{NH}_4\text{-N}$ from mangrove sediment in summer as a result of increased ammonium uptake. In contrast, the low primary production and weak microbial activity in spring (due to lower temperature) facilitated accumulation of $\text{NH}_4\text{-N}$ and lower removal of $\text{NO}_3\text{-N}$, leading to relatively high $\text{NH}_4\text{-N}$ efflux and low $\text{NO}_3\text{-N}$ influx.

Terrigenous input, mineralization of organic matter, activation and release of iron-bound P are the main sources of DRP in mangrove sediments. Litterfall from mangrove trees has been considered an important source of organic matter to mangrove sediments (Alongi et al., 2005; Murdiyarto et al., 2015). Litterfall increases in summer (growing season) and reaches a maximum in fall, leading to much more deposition of organic matter into the surface sediments (Chen et al., 2009; Robert et al., 2017). Strong mineralization in summer would transform more DOP to DRP, leading to a high inventory of DRP in mangrove sediments that is available to export. As a result, DRP was higher while DOP was lower during ebb tide in summer (Table S2), accompanied by a higher net export of DRP to estuary, while the net import of estuary DOP to mangrove increased (Fig. 5). This is consistent with a recent study which found that PO_4^{3-} in the intertidal aquifer had a larger inventory in summer than spring (Liu et al., 2018). In addition, iron-bound phosphate can be released into sediment porewater in reducing conditions (Smolders et al., 2017). The lower Eh of mangrove sediments observed in summer than spring (Wang et al., 2019a) suggested the likelihood of more sediment DRP export.

The seasonal changes in magnitude and direction of exchange fluxes indicate that the mangrove forest plays a dynamic role as a nutrient source or sink, thereby regulating the nutrient status of the estuary ecosystem. In summer cases, both $\text{NH}_4\text{-N}$ efflux and $\text{NO}_3\text{-N}$ influx increased but the combined result was a significant reduction of overall N (DIN and DTN) load to the estuary. In spring, mangroves were still a sink of DIN and DTN although the net influx was minor (Fig. 5). Mangroves are a stronger source of DRP in summer than spring, while DOP and DTP shifted from net export in spring to net import in summer, and mangroves were a strong sink for TP in spring due to high TPP retention.

4.3. The influence of upstream effluents on nutrient fluxes during ebb tides

Effluents discharged from upstream areas during ebb tide increased the efflux of $\text{NH}_4\text{-N}$, DON, DIN and DTN (Fig. 6). Effluents are always rich in $\text{NH}_4\text{-N}$, and this is recognized as the common cause of eutrophication in coastal areas (Queiroz et al., 2013; Kaiser et al., 2015). In our study area, $\text{NH}_4\text{-N}$ ($175.5 \pm 79.1 \mu\text{mol L}^{-1}$) in effluents were about 4 times higher than that in the tidal creek and

estuary ($38.7 \pm 24.1 \mu\text{mol L}^{-1}$) (Wang et al., 2019a). Briggs and Funge-Smith (1994) showed that only 24% of total nutrient can be transformed into biomass, and about 35% is discharged into coastal water without conversion. In addition, microbial activities and the decomposition of organic matter (formation and transformation of DON) are stronger in disturbed mangrove sediments receiving nutrient-rich effluents than in undisturbed sediments (Feller et al., 1999; Suarez-Abelenda et al., 2014). When effluents loading was high, $\text{NH}_4\text{-N}$, DON, DIN and DTN had a higher export from mangrove to estuary (Fig. 6).

Average concentration of $\text{NO}_3\text{-N}$ in sewage and aquaculture wastewater was far lower than that in tidal creek and estuary water in our study area (Wang et al., 2019a). As expected, the $\text{NO}_3\text{-N}$ fluxes with effluents were slightly lower (5% and 0.3%) than the fluxes without effluents in July 2016 and April 2017. One exception occurred in June 2018 when the flux with effluents was 15% higher than the fluxes without effluents, likely because the large addition of nitrate from effluents (largest flow rate of $5.97 \text{ m}^3 \text{ s}^{-1}$) overwhelmed dilution by the low $\text{NO}_3\text{-N}$ sediment porewater. Moreover, recent studies found that ammonia-oxidizing bacteria (AOB) in effluents was more abundant than that in water without effluents (Damashek et al., 2015; Lin et al., 2020). The higher $\text{NH}_4\text{-N}$ (substrate for nitrification) and warmer water temperature during ebb tide in June 2018 might have enhanced nitrification and contributed to the increase of $\text{NO}_3\text{-N}$.

The enriched-P effluents also had a significant influence on P fluxes to the estuary. Current results showed that DRP (the dominant form of TP) concentration in the effluent-affected period was $15.0 \pm 7.6 \mu\text{mol L}^{-1}$, about three times higher than the period without effluents ($4.8 \pm 0.9 \mu\text{mol L}^{-1}$) (Table S4). Other studies have also suggested that the labile, bioavailable and other fractionated P are higher in mangrove systems affected by aquaculture wastewater and domestic sewage compared to unaffected systems (Nobrega et al., 2014; Barcellos et al., 2019). Effluent P can be transported to coastal water directly, or temporally absorbed into vegetation and returned to mangrove sediments through degradation (Barcellos et al., 2019). Even though the concentration of DOP in effluents ($1.8 \mu\text{mol L}^{-1}$) was much lower than DRP, it was higher than the DOP of unaffected tidal creeks and estuary (about $0.5 \mu\text{mol L}^{-1}$) (Table S4). Consequently, effluent discharge increased DOP export from mangrove to estuary.

Effluents discharged from upstream areas during the ebb tide period substantially increased the export of most nutrient species when the flow rate was higher. The increase in nutrient fluxes was

associated with effluent discharge. The water flux during the effluent-affected period (ebb tide) in June 2018 ($5.97 \text{ m}^3 \text{ s}^{-1}$) was larger than in July 2016 ($3.63 \text{ m}^3 \text{ s}^{-1}$), and only a small quantity of effluents was discharged in April 2017 ($0.48 \text{ m}^3 \text{ s}^{-1}$). As a result, the effluents caused significant increases in DTN and TP fluxes in June 2018 (29% and 75% higher) and July 2016 (3% and 23% higher), but only a minor change occurred in April 2017 (Fig. 6).

Effluents discharged from upstream areas also changed the nutrient stoichiometry. High $\text{NH}_4\text{-N}$ in effluents resulted in 50% higher molar ratio of DIN: DRP (37 ± 6) in the effluent-affected period than that without effluents (Table S4). Changes in nutrient supply can alter the structure, function and primary productivity of coastal ecosystems (Lapointe et al., 2015, 2020; Maavara et al., 2020). Nitrogen enrichment in our study area may further stimulate P-limited phytoplankton blooms (Lapointe et al., 2015). Effluent discharged into the tidal creek also increased the ratios of $\text{NH}_4\text{-N}$: $\text{NO}_3\text{-N}$ and DIN: DON (Table S4). Phytoplankton species abundance and composition have been found to be influenced by the availability of $\text{NH}_4\text{-N}$ and $\text{NO}_3\text{-N}$ in both oceanic and estuarine systems (Kiteresi et al., 2012). A previous study reported that non-toxic blooms are more likely to occur in high DIN: DON conditions while toxic blooms are more likely to occur in low DIN: DON conditions (Hood et al., 2006). Therefore, the effluents have modified efflux from mangrove to estuary with changing stoichiometry, presenting important ecological effects on estuarine ecosystems.

5. Conclusions

This study provides a holistic perspective on lateral nutrient fluxes through the mangrove-estuary interface. A conceptual schematic of nutrient exchange between mangrove and estuary is illustrated in Fig. 7. The lateral fluxes of nutrient components suggest that mangroves always served as a source of $\text{NH}_4\text{-N}$ and DRP to the estuary, but as a sink of $\text{NO}_3\text{-N}$. Overall, mangroves were a net sink of DIN, DTN and TP, and this relationship is driven by tidal exchange and large nutrient retention by the mangrove ecosystem. Higher temperatures in summer (June and July) increases primary production (ammonium uptake) and microbial activities (nitrate denitrification), resulting in a lower export of $\text{NH}_4\text{-N}$ and higher import of $\text{NO}_3\text{-N}$ compared with spring (April). Strong mineralization likely transforms DOP to DRP in summer, as a result of which relatively more DRP and less DOP is exported to the estuary. DON, DOP and DTP shifted from net export (source) in spring to net import (sink) in summer due to the changing balance of P input and

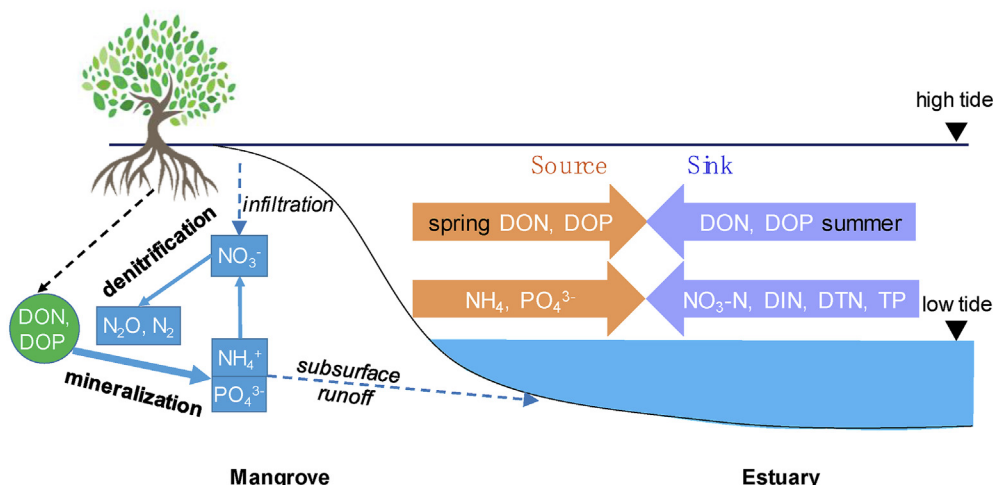


Fig. 7. Conceptual schematic of tidal driven nutrients exchange between mangrove and estuary showing a dynamic source-sink pattern.

biological and physicochemical processes. The discharge of upstream effluents during ebb tide substantially increased nutrient export, offsetting the role of mangrove on mitigating coastal eutrophication. The dynamic source-sink pattern of nutrient implied increasing mangrove coverage or controlling anthropogenic nutrient input can alleviate coastal eutrophication in this region. This study highlights the importance of an integrated land-ocean management of nutrient pollution and restoration of coastal wetlands.

Credit author statement

We confirm that this manuscript has not been published elsewhere and is not under consideration by another journal. All authors have approved the manuscript and agree with its submission to Chemosphere.

Declaration of competing interest

The authors declare that they have no known competing financial interests or personal relationships that could have appeared to influence the work reported in this paper.

Acknowledgments

This research was supported by the National Natural Science Foundation of China (No. 41976138), the National Key Research and Development Program of China (2016YFE0202100), the Key Laboratory of the Coastal and Wetland Ecosystems (WELRI201601), the State Key Laboratory of Marine Environmental Science (MELRI1603), and the Fundamental Research Funds for the Central Universities of China (20720180118). We thank Junou Du for her help in the analysis of nutrients, Chenjuan Zheng for her organizational help and all the students who assisted in fieldwork.

Appendix A. Supplementary data

Supplementary data to this article can be found online at <https://doi.org/10.1016/j.chemosphere.2020.128665>.

References

- Alongi, D.M., Boto, K.G., Robertson, A.I., 1992. Nitrogen and phosphorus cycles. In: Robertson, A.I., Alongi, D.M. (Eds.), *Tropical Mangrove Ecosystems*. American Geophysical Union, Washington, pp. 251–292. <https://doi.org/10.1029/CE041p0251>.
- Alongi, D.M., Pfizner, J., Trott, L.A., Tirendi, F., Dixon, P., Klumpp, D.W., 2005. Rapid sediment accumulation and microbial mineralization in forests of the mangrove *Kandelia candel* in the Jiulongjiang Estuary, China. *Estuar. Coast Shelf Sci.* 63, 605–618. <https://doi.org/10.1016/j.ecss.2005.01.004>.
- Atwood, T.B., Connolly, R.M., Almahasheer, H., Carnell, P.E., Duarte, C.M., Lewis, C.J.E., Irigoien, X., Kelleway, J.J., Lavery, P.S., Macreadie, P.I., Serrano, O., Sanders, C.J., Santos, I., Steven, A.D.L., Lovelock, C.E., 2017. Global patterns in mangrove soil carbon stocks and losses. *Nat. Clim. Change* 7, 523. <https://doi.org/10.1038/nclimate3326>.
- Barbier, E.B., Hacker, S.D., Kennedy, C., Koch, E.W., Stier, A.C., Silliman, B.R., 2011. The value of estuarine and coastal ecosystem services. *Ecol. Monogr.* 81, 169–193. <https://doi.org/10.1890/10-1510.1>.
- Barcellos, D., Queiroz, H.M., Nobrega, G.N., de Oliveira, R.L., Santaella, S.T., Otero, X.L., Ferreira, T.O., 2019. Phosphorus enriched effluents increase eutrophication risks for mangrove systems in northeastern Brazil. *Mar. Pollut. Bull.* 142, 58–63. <https://doi.org/10.1016/j.marpolbul.2019.03.031>.
- Bergamaschi, B.A., Krabbenhoft, D.P., Aiken, G.R., Patino, E., Rumbold, D.G., Orem, W.H., 2012. Tidally driven export of dissolved organic carbon, total mercury, and methylmercury from a mangrove-dominated estuary. *Environ. Sci. Technol.* 46, 1371–1378. <https://doi.org/10.1021/es2029137>.
- Briggs, M.R.P., Funge-Smith, S.J., 1994. A nutrient budget of some intensive marine shrimp ponds in Thailand. *Aquacult. Fish. Manag.* 25, 789–811. <https://doi.org/10.1111/j.1365-2109.1994.tb00744.x>.
- Call, M., Sanders, C.J., Macklin, P.A., Santos, I.R., Maher, D.T., 2019. Carbon outwelling and emissions from two contrasting mangrove creeks during the monsoon storm season in Palau, Micronesia. *Estuar. Coast Shelf Sci.* 218, 340–348. <https://doi.org/10.1016/j.ecss.2019.01.002>.
- Camacho-Valdez, V., Ruiz-Luna, A., Ghermandi, A., Nunes, P.A.L.D., 2013. Valuation of ecosystem services provided by coastal wetlands in northwest Mexico. *Ocean Coast Manag.* 78, 1–11. <https://doi.org/10.1016/j.ocecoaman.2013.02.017>.
- Chen, C., Beardsley, R., Cowles, G., 2006. An unstructured grid, finite-volume coastal ocean model (FVCOM) system. *Oceanography* 19, 78–89. <https://doi.org/10.5670/oceanog.2006.92>.
- Chen, G.C., Tam, N.F.Y., Wong, Y.S., Ye, Y., 2011. Effect of wastewater discharge on greenhouse gas fluxes from mangrove soils. *Atmos. Environ.* 45, 1110–1115. <https://doi.org/10.1016/j.atmosenv.2010.11.034>.
- Chen, L., Zan, Q., Li, M., Shen, J., Liao, W., 2009. Litter dynamics and forest structure of the introduced *Sonneratia caseolaris* mangrove forest in Shenzhen, China. *Estuar. Coast Shelf Sci.* 85, 241–246. <https://doi.org/10.1016/j.ecss.2009.08.007>.
- Damashek, J., Smith, J.M., Mosier, A.C., Francis, C.A., 2015. Benthic ammonia oxidizers differ in community structure and biogeochemical potential across a riverine delta. *Front. Microbiol.* 5, 18. <https://doi.org/10.3389/fmicb.2014.00743>.
- Dittmar, T., Hertkorn, N., Kattner, G., Lara, R.J., 2006. Mangroves, a major source of dissolved organic carbon to the oceans. *Global Biogeochem. Cycles* 20, 7. <https://doi.org/10.1029/2005gb002570>.
- Duan, P.P., Song, Y.F., Li, S.S., Xiong, Z., 2019. Responses of N₂O production pathways and related functional microbes to temperature across greenhouse vegetable field soils. *Geoderma* 355, 9. <https://doi.org/10.1016/j.geoderma.2019.113904>.
- Estoque, R.C., Myint, S.W., Wang, C.Y., Ishtiaque, A., Aung, T.T., Emerton, L., Ooba, M., Hijioka, Y., Mon, M.S., Wang, Z., Fan, C., 2018. Assessing environmental impacts and change in Myanmar's mangrove ecosystem service value due to deforestation (2000–2014). *Global Change Biol.* 24, 5391–5410. <https://doi.org/10.1111/gcb.14409>.
- Feller, I.C., Whigham, D.F., O'Neill, J.P., McKee, K.L., 1999. Effects of nutrient enrichment on within-stand cycling in a mangrove forest. *Ecology* 80, 2193–2205. [https://doi.org/10.1890/0012-9658\(1999\)080\[2193:Eoneow\]2.0.Co;2](https://doi.org/10.1890/0012-9658(1999)080[2193:Eoneow]2.0.Co;2).
- Field, C.D., 1995. Impact of expected climate-change on mangroves. *Hydrobiologia* 295, 75–81. <https://doi.org/10.1007/bf00029113>.
- Gleeson, J., Santos, I.R., Maher, D.T., Golsby-Smith, L., 2013. Groundwater-surface water exchange in a mangrove tidal creek: evidence from natural geochemical tracers and implications for nutrient budgets. *Mar. Chem.* 156, 27–37. <https://doi.org/10.1016/j.marchem.2013.02.001>.
- Hood, R.R., Zhang, X., Glibert, P.A., Roman, M.R., Stoecker, D.K., 2006. Modeling the influence of nutrients, turbulence and grazing on *Pfiesteria* population dynamics. *Harmful Algae* 5, 459–479. <https://doi.org/10.1016/j.hal.2006.04.014>.
- Hopkinson, C.S., Giblin, A.E., Tucker, J., Garritt, R.H., 1999. Benthic metabolism and nutrient cycling along an estuarine salinity gradient. *Estuaries* 22, 863–881. <https://doi.org/10.2307/1353067>.
- Kaiser, D., Kowalski, N., Böttcher, M.E., Bing, Y., Unger, D., 2015. Benthic nutrient fluxes from mangrove sediments of an anthropogenically impacted estuary in southern China. *J. Mar. Sci. Eng.* 3, 466–491. <https://doi.org/10.3390/jmse3020466>.
- Kaiser, D., Unger, D., Qiu, G.L., Zhou, H.L., Gan, H.Y., 2013. Natural and human influences on nutrient transport through a small subtropical Chinese estuary. *Sci. Total Environ.* 450, 92–107. <https://doi.org/10.1016/j.scitotenv.2013.01.096>.
- Kiteresi, L.I., Okuku, E.O., Mwangi, S.N., Ohowa, B., Wanjeri, V.O., Okumu, S., Mkono, M., 2012. The influence of land based activities on the phytoplankton communities of Shimoni-Vanga system, Kenya. *Int. J. Environ. Res.* 6, 151–162. [10.11089.131&rep=rep1&type=pdf](https://doi.org/10.11089.131&rep=rep1&type=pdf).
- Lapointe, B.E., Herren, L.W., Brewton, R.A., Alderman, P.K., 2020. Nutrient over-enrichment and light limitation of seagrass communities in the Indian River Lagoon, an urbanized subtropical estuary. *Sci. Total Environ.* 699, 15. <https://doi.org/10.1016/j.scitotenv.2019.134068>.
- Lapointe, B.E., Herren, L.W., Debortoli, D.D., Vogel, M.A., 2015. Evidence of sewage-driven eutrophication and harmful algal blooms in Florida's Indian River Lagoon. *Harmful Algae* 43, 82–102. <https://doi.org/10.1016/j.hal.2015.01.004>.
- Lee, S., Cho, K., Lim, J., Kim, W., Hwang, S., 2011. Acclimation and activity of ammonia-oxidizing bacteria with respect to variations in zinc concentration, temperature, and microbial population. *Bioresour. Technol.* 102, 4196–4203. <https://doi.org/10.1016/j.biortech.2010.12.035>.
- Lin, J.J., Chen, N.W., Wang, F.F., Huang, Z.Y., Zhang, X.Y., Liu, L., 2020. Urbanization increased river nitrogen export to western Taiwan Strait despite increased retention by nitrification and denitrification. *Ecol. Indic.* 109, 10. <https://doi.org/10.1016/j.ecolind.2019.105756>.
- Liu, M.Y., Li, H.Y., Li, L., Man, W.D., Jia, M.M., Wang, Z.M., Lu, C.Y., 2017. Monitoring the invasion of spartina alterniflora using multi-source high-resolution imagery in the Zhangjiang estuary, China. *Rem. Sens.* 9, 18. <https://doi.org/10.3390/rs9060539>.
- Liu, Y., Liang, W.Z., Jiao, J.J., 2018. Seasonality of nutrient flux and biogeochemistry in an intertidal aquifer. *J. Geophys. Res.-Oceans* 123, 6116–6135. <https://doi.org/10.1029/2018jc014197>.
- Maavara, T., Akbarzadeh, Z., Van Cappellen, P., 2020. Global dam-driven changes to riverine N:P:Si ratios delivered to the coastal ocean. *Geophys. Res. Lett.* 47. <https://doi.org/10.1029/2020gl088288>.
- Maher, D.T., Santos, I.R., Golsby-Smith, L., Gleeson, J., Eyre, B.D., 2013. Groundwater-derived dissolved inorganic and organic carbon exports from a mangrove tidal creek: the missing mangrove carbon sink? *Limnol. Oceanogr.* 58, 475–488. <https://doi.org/10.4319/lo.2013.58.2.0475>.
- Maie, N., Pisani, O., Jaffe, R., 2008. Mangrove tannins in aquatic ecosystems: their fate and possible influence on dissolved organic carbon and nitrogen cycling.

- Limnol. Oceanogr. 53, 160–171. <https://doi.org/10.4319/lo.2008.53.1.0160>.
- Molnar, N., Welsh, D.T., Marchand, C., Deborde, J., Meziane, T., 2013. Impacts of shrimp farm effluent on water quality, benthic metabolism and N-dynamics in a mangrove forest (New Caledonia). *Estuar. Coast Shelf Sci.* 117, 12–21. <https://doi.org/10.1016/j.ecss.2012.07.012>.
- Munksgaard, N.C., Hutley, L.B., Metcalfe, K.N., Padovan, A.C., Palmer, C., Gibb, K.S., 2019. Environmental challenges in a near-pristine mangrove estuary facing rapid urban and industrial development: Darwin Harbour, Northern Australia. *Reg. Stud. Mar. Sci.* 25, 15. <https://doi.org/10.1016/j.rsma.2018.11.001>.
- Murdiyasar, D., Purbopuspito, J., Kauffman, J.B., Warren, M.W., Sasmito, S.D., Donato, D.C., Manuri, S., Krisnawati, H., Taberima, S., Kurnianto, S., 2015. The potential of Indonesian mangrove forests for global climate change mitigation. *Nat. Clim. Change* 5, 1089–1092. <https://doi.org/10.1038/nclimate2734>.
- Nobrega, G.N., Otero, X.L., Macias, F., Ferreira, T.O., 2014. Phosphorus geochemistry in a Brazilian semiarid mangrove soil affected by shrimp farm effluents. *Environ. Monit. Assess.* 186, 5749–5762. <https://doi.org/10.1007/s10661-014-3817-3>.
- Paerl, H.W., Gardner, W.S., Havens, K.E., Joyner, A.R., McCarthy, M.J., Newell, S.E., Qin, B.Q., Scott, J.T., 2016. Mitigating cyanobacterial harmful algal blooms in aquatic ecosystems impacted by climate change and anthropogenic nutrients. *Harmful Algae* 54, 213–222. <https://doi.org/10.1016/j.hal.2015.09.009>.
- Perera, K., Amarasinghe, M.D., 2019. Carbon sequestration capacity of mangrove soils in micro tidal estuaries and lagoons: a case study from Sri Lanka. *Geoderma* 347, 80–89. <https://doi.org/10.1016/j.geoderma.2019.03.041>.
- Queiroz, H.M., Artur, A.G., Taniguchi, C.A.K., da Silveira, M.R.S., do Nascimento, J.C., Nobrega, G.N., Otero, X.L., Ferreira, T.O., 2019. Hidden contribution of shrimp farming effluents to greenhouse gas emissions from mangrove soils. *Estuar. Coast Shelf Sci.* 221, 8–14. <https://doi.org/10.1016/j.ecss.2019.03.011>.
- Queiroz, L., Rossi, S., Meireles, J., Coelho, C., 2013. Shrimp aquaculture in the federal state of Ceara, 1970–2012: trends after mangrove forest privatization in Brazil. *Ocean Coast Manag.* 73, 54–62. <https://doi.org/10.1016/j.ocecoaman.2012.11.009>.
- Reis, C.R.G., Nardoto, G.B., Oliveira, R.S., 2017. Global overview on nitrogen dynamics in mangroves and consequences of increasing nitrogen availability for these systems. *Plant Soil* 410, 1–19. <https://doi.org/10.1007/s11104-016-3123-7>.
- Robert, R.T., Edward, C.M., Victor, H.R.M., Andre, R., 2017. Productivity and carbon dynamics in mangrove wetlands. In: *Mangrove Ecosystems: A Global Biogeographic Perspective*. Springer, pp. 127–128. https://doi.org/10.1007/978-3-319-62206-4_5.
- Sadat-Noori, M., Glamore, W., 2019. Porewater exchange drives trace metal, dissolved organic carbon and total dissolved nitrogen export from a temperate mangrove wetland. *J. Environ. Manag.* 248, 11. <https://doi.org/10.1016/j.jenvman.2019.109264>.
- Santos, I.R., Maher, D.T., Larkin, R., Webb, J.R., Sanders, C.J., 2019. Carbon outwelling and outgassing vs. burial in an estuarine tidal creek surrounded by mangrove and saltmarsh wetlands. *Limnol. Oceanogr.* 64, 996–1013. <https://doi.org/10.1002/lno.11090>.
- Servais, S., Kominoski, J.S., Davis, S.E., Gaiser, E.E., Pachon, J., Troxler, T.G., 2019. Effects of nutrient-limitation on disturbance recovery in experimental mangrove wetlands. *Wetlands* 39, 337–347. <https://doi.org/10.1007/s13157-018-1100-z>.
- Smolders, E., Baetens, E., Verbeeck, M., Nawara, S., Diels, J., Verdier, M., Peeters, B., De Cooman, W., Bakens, S., 2017. Internal loading and redox cycling of sediment iron explain reactive phosphorus concentrations in lowland rivers. *Environ. Sci. Technol.* 51, 2584–2592. <https://doi.org/10.1021/acs.est.6b04337>.
- Songsom, V., Koedsin, W., Ritchie, R.J., Huete, A., 2019. Mangrove phenology and environmental drivers derived from remote sensing in Southern Thailand. *Rem. Sens.* 11, 25. <https://doi.org/10.3390/rs11080955>.
- Suarez-Abelenda, M., Ferreira, T.O., Camps-Arbestain, M., Rivera-Monroy, V.H., Macias, F., Nobrega, G.N., Otero, X.L., 2014. The effect of nutrient-rich effluents from shrimp farming on mangrove soil carbon storage and geochemistry under semi-arid climate conditions in northern Brazil. *Geoderma* 213, 551–559. <https://doi.org/10.1016/j.geoderma.2013.08.007>.
- Taillardat, P., Ziegler, A.D., Friess, D.A., Widory, D., Vinh Truong, V., David, F., Thanh-Nho, N., Marchand, C., 2018. Carbon dynamics and inconstant porewater input in a mangrove tidal creek over contrasting seasons and tidal amplitudes. *Geochim. Cosmochim. Acta* 237, 32–48. <https://doi.org/10.1016/j.gca.2018.06.012>.
- Valiela, I., Elmstrom, E., Lloret, J., Stone, T., Camilli, L., 2018. Tropical land-sea couplings: role of watershed deforestation, mangrove estuary processing, and marine inputs on N fluxes in coastal Pacific Panama. *Sci. Total Environ.* 630, 126–140. <https://doi.org/10.1016/j.scitotenv.2018.02.189>.
- Wang, F.F., Chen, N.W., Yan, J., Lin, J.J., Guo, W.D., Cheng, P., Liu, Q., Huang, B.Q., Tian, Y., 2019a. Major processes shaping mangroves as inorganic nitrogen sources or sinks: insights from a multidisciplinary study. *J. Geophys. Res.-Biogeosci.* 124, 1194–1208. <https://doi.org/10.1029/2018jg004875>.
- Wang, M., Zhang, J.H., Tu, Z.G., Gao, X.Q., Wang, W.Q., 2010. Maintenance of estuarine water quality by mangroves occurs during flood periods: a case study of a subtropical mangrove wetland. *Mar. Pollut. Bull.* 60, 2154–2160. <https://doi.org/10.1016/j.marpolbul.2010.07.025>.
- Wang, W.Q., Sardans, J., Wang, C., Zeng, C.S., Tong, C., Chen, G.X., Huang, J.F., Pan, H.R., Peguero, G., Vallicrosa, H., Penuelas, J., 2019b. The response of stocks of C, N, and P to plant invasion in the coastal wetlands of China. *Global Change Biol.* 25, 733–743. <https://doi.org/10.1111/gcb.14491>.
- Weston, N.B., Giblin, A.E., Banta, G.T., Hopkinson, C.S., Tucker, J., 2010. The effects of varying salinity on ammonium exchange in estuarine sediments of the Parker River, Massachusetts. *Estuar. Coasts* 33, 985–1003. <https://doi.org/10.1007/s12237-010-9282-5>.
- Whitehead, P.G., Crossman, J., 2012. Macronutrient cycles and climate change: Key science areas and an international perspective. *Sci. Total Environ.* 434, 13–17. <https://doi.org/10.1016/j.scitotenv.2011.08.046>.
- Xiao, K., Wu, J.P., Li, H.L., Hong, Y.G., Wilson, A.M., Jiao, J.J., Shanahan, M., 2018. Nitrogen fate in a subtropical mangrove swamp: potential association with seawater-groundwater exchange. *Sci. Total Environ.* 635, 586–597. <https://doi.org/10.1016/j.scitotenv.2018.04.143>.
- Zhang, X., Lin, C.Y., Zhou, X.L., Lei, K., Guo, B.B., Cao, Y.X., Lu, S., Liu, X.T., He, M.C., 2019. Concentrations, fluxes, and potential sources of nitrogen and phosphorus species in atmospheric wet deposition of the Lake Qinghai Watershed, China. *Sci. Total Environ.* 682, 523–531. <https://doi.org/10.1016/j.scitotenv.2019.05.224>.
- Zhang, Y., Wang, W., Wu, Q., Fang, B., Peng, L., 2006. The growth of *Kandelia candel* seedlings in mangrove habitats of the Zhangjiang estuary in Fujian, China. *Acta Ecol. Sin.* 26, 1648–1655. [https://doi.org/10.1016/S1872-2032\(06\)60028-0](https://doi.org/10.1016/S1872-2032(06)60028-0).
- Zheng, X.W., Guo, J.M., Song, W.M., Feng, J.X., Lin, G.H., 2018. Methane emission from mangrove wetland soils is marginal but can be stimulated significantly by anthropogenic activities. *Forests* 9, 13. <https://doi.org/10.3390/f9120738>.
- Zhou, H.C., Wei, S.D., Qi, Z., Zhang, L.H., Tam, N.F., Lin, Y.M., 2010. Nutrient and caloric dynamics in *Avicennia marina* leaves at different developmental and decay stages in Zhangjiang River Estuary, China. *Estuar. Coast Shelf Sci.* 87, 21–26. <https://doi.org/10.1016/j.ecss.2009.12.005>.